ORIGINAL PAPER

CrossMark

Preparation and characterization of nanocomposites based on different zeolite frameworks as carriers for anticancer drug: zeolite Y versus ZSM-5

M. Karimi[1] · M. Habibizadeh[2,3] · K. Rostamizadeh[2,4] · M. Khatamian[1] · B. Divband[5,6]

Abstract

This research was to investigate and characterize different types of zeolites, i.e., Y and ZSM-5 as well as their corresponding nanocomposite of PEG (PEG/Y and PEG/ZSM-5), as carrier for loading and release of curcumin. Zeolites and PEG/zeolite nanocomposites were characterized by XRD, SEM and FT-IR techniques. Curcumin encapsulation efficiency of zeolite Y, ZSM-5, PEG/Y and PEG/ZSM-5 was determined to be 61.06, 40.45, 45.59 and 37.76%, respectively. Nitrogen adsorption–desorption measurement was used to measure the surface area and the pore volume of the hosts before and after curcumin loading. The decrease in surface areas and pore volumes after drug loading was attributed to the inclusion of curcumin in the zeolites pores. In vitro drug release of curcumin was studied in buffer solution (pH = 5.4 and 7.4) at 37 °C. The results showed higher levels of curcumin release from zeolite Y compared to ZSM-5. The zeolite nanocomposites also revealed the higher level of released curcumin in comparison with the corresponding zeolites. The amount of curcumin released at pH = 5.4 was higher than at pH = 7.4, which can be used as evidence to demonstrate the pH sensitivity of the zeolite as drug carrier. From the results, it can be concluded that zeolite-based drug delivery systems can be considered as promising candidate for delivery of hydrophobic drugs such as curcumin.

✉ K. Rostamizadeh
rostamizadeh@zums.ac.ir; Rostamizadeh@gmail.com

1   Department of Inorganic Chemistry, Faculty of Chemistry, University of Tabriz, Tabriz, Iran

2   Department of Pharmaceutical Biomaterials, School of Pharmacy, Zanjan University of Medical Sciences, Zanjan, Iran

3   Student Research Committee, Zanjan University of Medical Sciences, Zanjan, Iran

4   Zanjan Pharmaceutical Nanotechnology Research Center, School of Pharmacy, Zanjan University of Medical Sciences, Zanjan, Iran

5   Dental and Periodontal Research Center, Tabriz University of Medical Sciences, Tabriz, Iran

6   Infectious and Tropical Diseases Research Center, Tabriz University of Medical Sciences, Tabriz, Iran

Introduction

Cancer, the most death cause in the world, attracts the most attention of researchers in the way to find new therapeutics for efficient treatment meanwhile avoid adverse side effects.

Curcumin (1,7-bis(4-hydroxy-3-methoxyphenyl)-1,6-heptadiene-3,5-dione) has recently attracted a great deal of attention because of biological and pharmacological activities, including antioxidant, anti-inflammatory, anti-tumor, anticarcinogenic, antimicrobial, anti-HIV activities. Curcumin is a lipophilic polyphenolic compound which is isolated from the rhizome of the herb Curcuma longa and shows low intrinsic toxicity and high therapeutic efficacy, but suffers from low water solubility and stability, and poor oral bioavailability which consequently limit its applications. To overcome these shortcomings, some studies have been focused on developing a suitable delivery system, such as liposomes, nano- or micro-emulsions, polymeric nanoparticles and solid lipid nanoparticles, in order to improve the stability and bioavailability of curcumin.

Inorganic/polymer nanocomposite materials have received significant interest due to the wide range of potential applications [1–5]. Zeolites are microporous inorganic crystalline materials with a three-dimensional framework consisting of silicon, aluminum and oxygen. They have many advantages such as well-defined pore structure, tunable base–acid sites, molecular sieve, and ion exchange capabilities [6]. Up to now different types of zeolites have been discovered and synthesized. They are classified according to the differences in the framework structure, Si/Al ratio, pore size, hydrophilicity, etc. They have been used for variety of applications, i.e., adsorption, catalysis, separation [2]. They also have wide range of applications in drug delivery systems due to properties such as biocompatibility, nontoxicity and high capacity in drug encapsulation, and dual functional surface (external and internal) [7, 8]. For instance, zeolite Y has been used to produce controllable release dosage of anthelmintic drugs and sustained release capsules of ibuprofen [9, 10]. Diclofenac sodium and piroxicam were used as drug models for being loaded into zeolites X and Y as the carriers [11]. Amorim et al. studied the characteristic of two different structures of zeolites, faujasite (FAU) and Linde type A (LTA), as carrier for α-cyano-4-hydroxycinnamic acid (CHC). The findings revealed that both the zeolites showed no toxicity toward HCT-15 (human colon carcinoma) cell line viability. On the other hand, CHC-loaded zeolites inhibited cell viability up to 585-fold, as compared to the free drug [12].

In contrast to zeolite's benefits in drug delivery, the application of these materials as carrier for drug delivery systems is associated with some problems. One of the major problems is that it is difficult to control drug release, which occurs mainly by diffusion. This is mainly because of their pore sizes which are notably larger than those of some drugs. To overcome this shortcoming and for a better control of drug delivery, the pore size should be adjusted to the drug dimension. This may be achieved by decreasing the pore size by anchoring functional groups

on the pore walls or synthesis materials with lower pore diameter. It has been shown that drug delivery becomes slower as the pore diameter of MCM-41-type silica decreases [13]. Besides, zeolites due to their surface hydrophilic properties suffer from low loading capacity. The approach to solving this problem can be the surface modification of zeolites with various surfactants and polymers [14, 15]. The presence of surfactants on solid surfaces and the formation of nanocomposites can induce or enhance the co-adsorption of different organic molecules, due to the variation of the hydrophilic characteristic of the substrate [16]. Thus, modification of natural zeolites with a surface-modifying agent provides the possibility to adsorb various bioactive agents, while retaining favorable hydraulic properties and providing a high affinity for drug molecules. The surface modification of zeolites can be achieved chemically or physically. In case of chemical surface modification, the hydroxyl groups on the surface provide the possibility to link the variety of materials to improve their characteristics as carrier. The surface hydroxyl groups of zeolite Y were modified with 1,1,3,3-tetramethyldisilazane, $HN(SiHMe_2)_2$ and encapsulated paraquat (methyl viologen) [17]. The results showed that the surface modification caused the equilibration time to be extended up to 7 days. Serri et al. [16] have introduced surface-modified natural zeolite (SMNZ) with cationic surfactant in order to improve the loading of diclofenac sodium through ionic interactions. The finding showed that the granules composed of SMNZ meet requirements for an oral dosage form, e.g., suitable dosage uniformity, a proper flowability, controlled drug delivery, and low cytotoxicity. They induced a prolonged anti-inflammatory effect on RAW264.7 cells as well.

The aim of this work is to investigate the influence of PEG as a surface-modifying agent on the properties of two types of zeolite, i.e., zeolite Y and ZSM-5, as carrier for curcumin. PEG/zeolite nanocomposites were considered due to nontoxicity and biocompatibility of PEG which could improve the properties of zeolite as delivery system. Then, the zeolites and their nanocomposites were characterized by FT-IR, XRD and TGA methods. We investigated loading and release of curcumin from pure zeolite and zeolite nanocomposites (PEG/Y and PEG/ZSM-5). In vitro drug release of curcumin was also studied in two different buffered solutions (pH 7.4 and 5.4).

Experimental

Materials

Zeolite Y and ZSM-5 were supplied by Azar Kimia Khatam Knowledge Based company (Tabriz, Iran) as powder. The activation of the zeolites (ZSM-5 and Y) was carried out at 120 °C for 24 h in order to remove the physisorbed water from the zeolites, resulting in a high surface area and accessible pore volume. PEG6000 was obtained from Kimiagarane Emrouz (Iran). Ethyl acetate was supplied by Amertat Shimi (Iran), and ethanol was obtained from Kimia Alcohol (Zanjan, Iran). Curcumin, Na_2HPO_4 and NaH_2PO_4 were from Merck (Germany) and purchased locally.

Preparation of PEG/zeolites nanocomposites (PEG/Y and PEG/ZSM-5)

The PEG-modified zeolites (PEG/ZSM-5 and PEG/Y) were prepared by mixing 125 mg of PEG and 500 mg of each zeolite in 20 ml of ethyl acetate under magnetic stirring at the speed of 600 rpm at 60 °C for 8 h, followed by solvent evaporation in petri dish for at least 24 h at room temperature [18].

Characterization

X-ray diffraction patterns (XRD)

X-ray diffraction patterns (XRD) were collected using a Siemens D500 diffractometer with Cu kα radiation ($\lambda = 1.5418$ A and $2\Theta = 4$–70) at room temperature.

FT-IR spectroscopy

Fourier transform infrared spectroscopy (FT-IR spectroscopy) is commonly used as an analytical technique to identify different materials and also to study their interaction with each other. FT-IR spectra of the samples in KBr pellets were measured using Bruker Model Tensor 27 equipment in the range of 4000–400 cm^{-1}.

Thermogravimetric analysis (TGA)

Thermogravimetric analysis (TGA) was performed on NETZSCH STA 409 PC/PG equipment, under nitrogen atmosphere. The samples were heated from room temperature to 800 °C with a heating rate of 10 °C/min, and the weight changes were recorded. The TGA data were used to confirm the successful surface modification of zeolites and to calculate the extent of curcumin loading on the zeolites and their corresponding nanocomposites.

Zeta potential analysis

In order to determine the surface charge of various species, the zeta potential of all samples was determined by photon correlation spectroscopy using a Nano-Zetasizer (Malvern Instruments, Nano ZS, Worcestershire, UK) working on the dynamic light scattering (DLS) platform equipped with a standard 633-nm laser.

Nitrogen adsorption isotherm

Nitrogen adsorption isotherm was determined at 77k with a Belsorp instrument. The samples were previously outgassed at 120 °C under vacuum. The specific surface area

was calculated by the BET method, and the total pore volume (V_{total}) was estimated from N_2 amount adsorbed at a relative pressure of 0.990 P/P°.

Scanning electron microscope

Scanning electron microscope (SEM, TECAN MIR3 FEG) was used to observe the morphology of the zeolites and nanocomposites. The samples were gold-coated prior to examination.

Measurement of free radical scavenging activity

The determination of scavenging activity with DPPH is a common method to evaluate the free radical scavenging ability of various compounds. In this study, the influence of curcumin encapsulation in Y, ZSM-5, PEG/Y and PEG/ZSM-5 zeolites on the free radical scavenging activity of curcumin was investigated. The radical scavenging activity of curcumin was determined according to the previous method [19]. Briefly, the different concentrations of curcumin were prepared in methanol (0.006–0.06 mM) while being protected from light. Equal volume of each curcumin solution was added to the DPPH solution (100 mM), and absorbance was recorded at 517 nm after 30 min. Triplicate experiments were performed for each sample. Scavenging activity was calculated using the following formula:

$$\text{DPPH radical scavenging activity}(\%) = \frac{A_C - A_S}{A_C} \times 100,$$

where A_C stands for the absorbance of the control and A_S is the absorbance of drug solution.

Host–guest system preparation

Different zeolites including zeolite Y, ZSM-5, PEG/Y and PEG/ZSM-5 were considered as host for the encapsulation of curcumin by a soaking procedure. Briefly, 500 mg of desired host, i.e., ZSM-5, Y, PEG/ZSM-5 and PEG/Y, was mixed with curcumin dissolved in ethanol (2 mg/mL) and stirred for 48 h at room temperature. During this time, the original white color of host changed to yellow, indicating the location of curcumin in the host sites. Then, the solution was centrifuged for 20 min at 14,000 rpm. The products were dried in an oven at 60 °C for 12 h. The extent of curcumin encapsulation in carriers was calculated considering the absorption of supernatant at $\lambda = 418$ nm by UV–visible spectrophotometer (Jenway 6305). Encapsulation efficiency of curcumin was determined as follows:

$$\text{Encapsulation efficiency}(\%) = \frac{\text{total feed drug} - \text{unencapsulated drug}}{\text{total feed drug}} \times 100.$$

In vitro drug release study

The release of curcumin from zeolite structures was studied in PBS containing 0.5% (w/v) Tween 80 in physiological pH of 7.4 and acidic media with the pH value of 5.4. Typically, 15 mg of desired curcumin-loaded host (i.e., Y, ZSM-5, PEG/Y and PEG/ZSM-5) was placed into a dialysis bag (cutoff 12 kDa) and introduced to 20 mL of PBS with desired pH under stirring at 37 °C. At predetermined time intervals, in order to determine the drug concentration in dialysate and consequently time-dependent drug release profile, 1.0 mL of dialysate was taken out and replaced with 1.0 mL of fresh buffer solution maintained at 37 °C and assayed by UV–Vis spectroscopy at $\lambda = 418$ nm.

Drug release kinetic

In order to evaluate in vitro drug release mechanism, different mathematical models were applied to represent the data obtained in the release experiments of different carriers, i.e., ZSM-5, PEG/ZSM-5, Y and PEG/Y. In this work, the data were analyzed using zero-order model, first-order model, second-order model, Higuchi model, Hixson–Crowell model, Korsmeyer–Peppas model and Kopcha model.

Results and discussion

X-ray diffraction analysis

X-ray diffraction analysis is one of the simplest and commonly used techniques for characterization of a zeolite structure. The data derived from X-ray diffraction analysis could provide valuable information about sample purity and/or evidence of consistency with a known structure. It also gives some information about the surface characteristics of different samples. Figure 1a shows the powder X-ray diffraction (XRD) patterns of ZSM-5, PEG, PEG/ZSM-5 and curcumin-loaded nanocomposites. The XRD pattern of ZSM-5 is similar to standard MFI structure reported for ZSM-5 zeolites [20]. XRD pattern for PEG indicates reflections at $2\Theta = 19.22$, 23.34 as reported in other studies [21–25]. Both characteristic peaks of ZSM-5 and PEG appeared at XRD pattern for PEG/ZSM-5 nanocomposite. However, being PEG in PEG/ZSM-5 structure results in a little change in the distance between the crystal layers of ZSM-5 zeolite which can be considered as evidence for successful synthesis of PEG/ZSM-5 nanocomposite. In addition, the similarity between XRD diffraction pattern of curcumin-loaded PEG/ZSM-5 and the one of PEG/ZSM-5 nanocomposite suggests that the nanocomposite structure is well preserved during the curcumin loading.

XRD pattern of Y zeolite, PEG/Y and curcumin-loaded PEG/Y are shown in Fig. 1b. Clearly, the XRD pattern for Y zeolite corresponds with FAU structure according to the previous report [26]. The peaks of PEG in the XRD pattern of
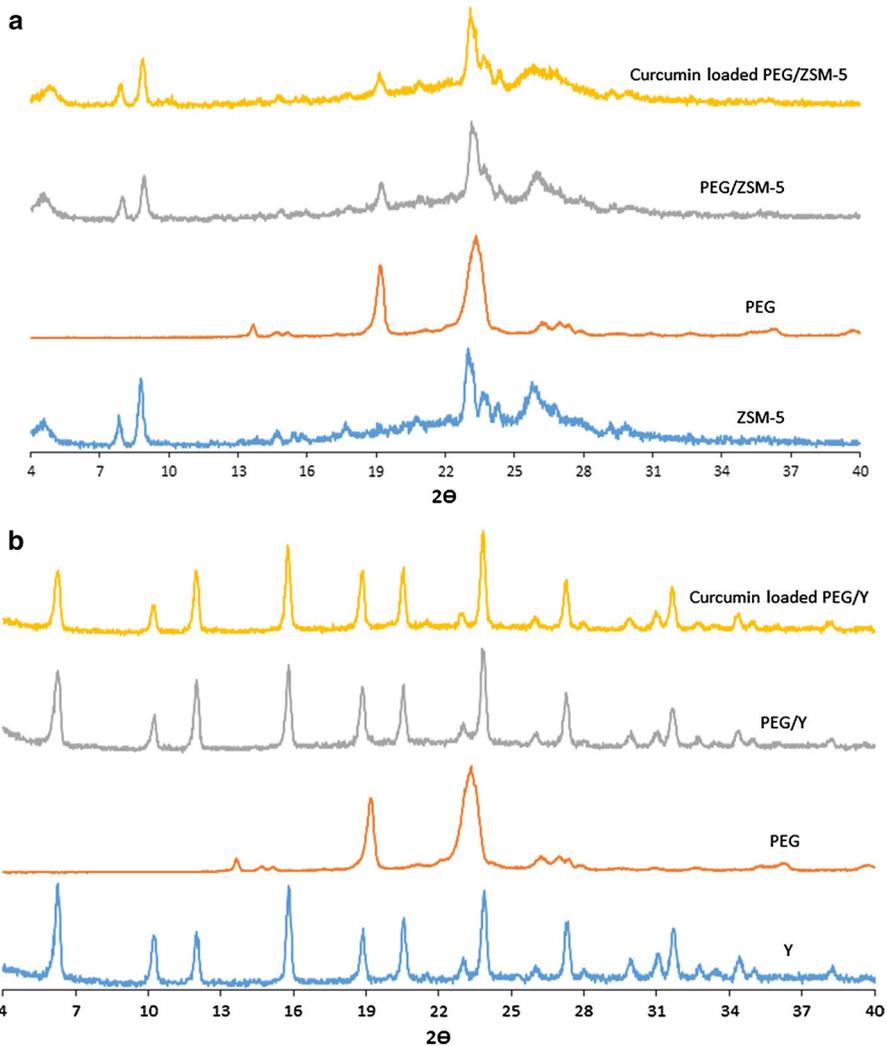
Fig. 1 XRD patterns for: **a** ZSM-5, PEG, PEG/ZSM-5, curcumin-loaded PEG/ZSM-5; **b** Y, PEG, PEG/Y, curcumin-loaded PEG/Y

PEG/Y did not appear presumably due to their overlap with Y zeolite peaks. However, the distance between the crystal layers and the intensity of the XRD peaks in PEG/Y slightly changed compared to the Y zeolite because of the PEG presence in the nanocomposite structure. On the other hand, the result of the drug-loaded PEG/Y does not show any change in the peak pattern, indicating that drug loading in PEG/Y did not have any significant changes on the nano-composite structure.
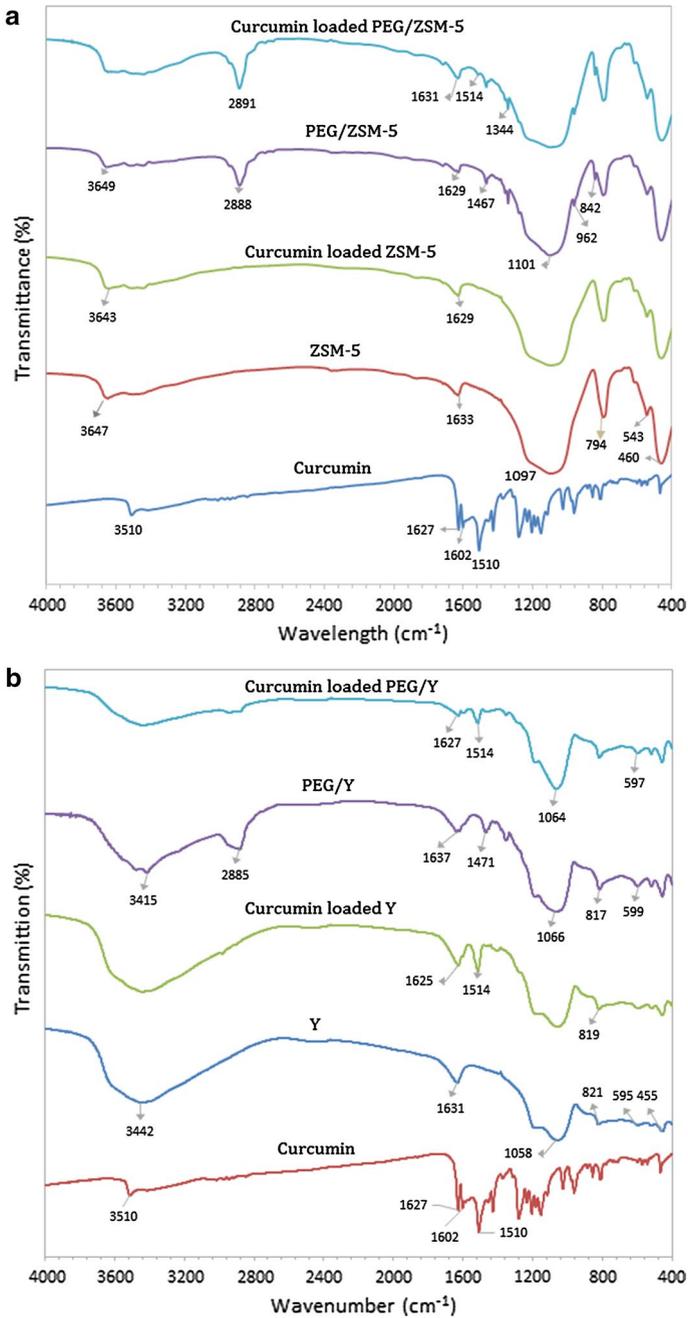
Fig. 2 FT-IR for: **a** curcumin, ZSM-5, curcumin-loaded ZSM-5, PEG/ZSM-5, curcumin-loaded PEG/ZSM-5; **b** curcumin, Y, curcumin-loaded Y, PEG/Y, curcumin-loaded PEG/Y

FT-IR spectroscopy

FT-IR spectroscopy provides the evidence of molecular-level interactions of the guest (curcumin) with the host (zeolite). The FT-IR spectrum was analyzed to probe the successful synthesis of PEG-modified zeolites and to evaluate the drug interaction. FT-IR spectra of curcumin, ZSM-5, curcumin-loaded ZSM-5, PEG/ZSM-5 and curcumin-loaded PEG/ZSM-5 are shown in Fig. 2a. In Fig. 2, for curcumin spectrum, the band at 3510 cm^{-1} is related to stretching vibration of the curcumin's phenol groups and the peaks at 1627 and 1602 cm^{-1} can be ascribed to the double bond C=C and the aromatic double bond C=C in the curcumin structure, respectively [27]. Figure 2 shows the FT-IR spectrum of ZSM-5 zeolite. The peak at 460 cm^{-1} corresponds to T–O bending vibration of the T–O_4 internal tetrahedral [28]. Absorbance peak at 543 cm^{-1} is related to the presence of the double ring (D_5R), in the framework structure. The peaks in 700 and 794 cm^{-1} can be attributed to the symmetric stretching vibration of internal TO_4 tetrahedral and external tetrahedral connections, respectively [29]. The peak at 1097 cm^{-1} is assigned to internal asymmetric stretching vibration of T–O [30], and the peaks at 1633 and 3637 cm^{-1} result from bending and stretching vibrations of adsorbed water molecules, respectively.

Figure 2a shows FT-IR spectrum of curcumin-loaded ZSM-5. As it can be seen, curcumin absorption bands cannot be distinguished probably because of overlapping with ZSM-5 absorption bands; however, the shifts in the absorption bands of ZSM-5 zeolite from 1633 to 1629 cm^{-1} and 3647 to 3643 cm^{-1} can be indicative of the drug loading and interaction with the ZSM-5 zeolites.

The spectrum of PEG/ZSM-5 nanocomposite shows the absorbance bands at 2888 and 1467 cm^{-1} which are related to the stretching and bending vibrations of CH_2 groups of PEG, and the peaks at 962 and 842 cm^{-1} are assigned to the stretching vibration of C–C [31]. This spectrum confirms the formation of PEG/ZSM-5 nanocomposite, because it has not only absorbance peaks of ZSM-5, but also absorbance peaks of PEG and it also shows a shift in the absorbance bands of ZSM-5 zeolite from 1097 to 1101 cm^{-1}, 1633 to 1629 cm^{-1} and 3647 to 3649 cm^{-1}.

As shown in Fig. 2a, the curcumin absorbance bands in the curcumin-loaded PEG/ZSM-5 spectrum were not observed again presumably because of overlapping with ZSM-5 peaks, but there is a little shift in the PEG/ZSM-5 nanocomposites absorbance bands.

Figure 3b shows FT-IR spectrum for the Y zeolite, curcumin-loaded Y zeolite, PEG/Y nanocomposites and curcumin-loaded PEG/Y. In Y zeolite spectrum, the vibration peaks at 455 and 595 cm^{-1} are because of internal bending vibrations of TO_4 and double rings (D_6R) and the peaks at 821 and 1058 cm^{-1} are related to symmetric and asymmetric stretching vibrations [28]. The presence of curcumin in the Y zeolite structure shifts the Y zeolite absorption bands from 1631 to 1625 cm^{-1} and 821 to 819 cm^{-1} confirming the successful curcumin loading in the Y zeolite.

The appearance of characteristic absorption peaks of PEG as well as a bite shift in the Y zeolite absorption bands in PEG/Y spectrum confirms the successful preparation of the PEG/Y nanocomposites. After curcumin loading into PEG/Y nanocomposite, nanocomposites absorption bands are shifted from 599 to 597 cm^{-1}, 1066 to 1064 cm^{-1} and 1637 to 1627 cm^{-1}, indicating the successful drug loading.
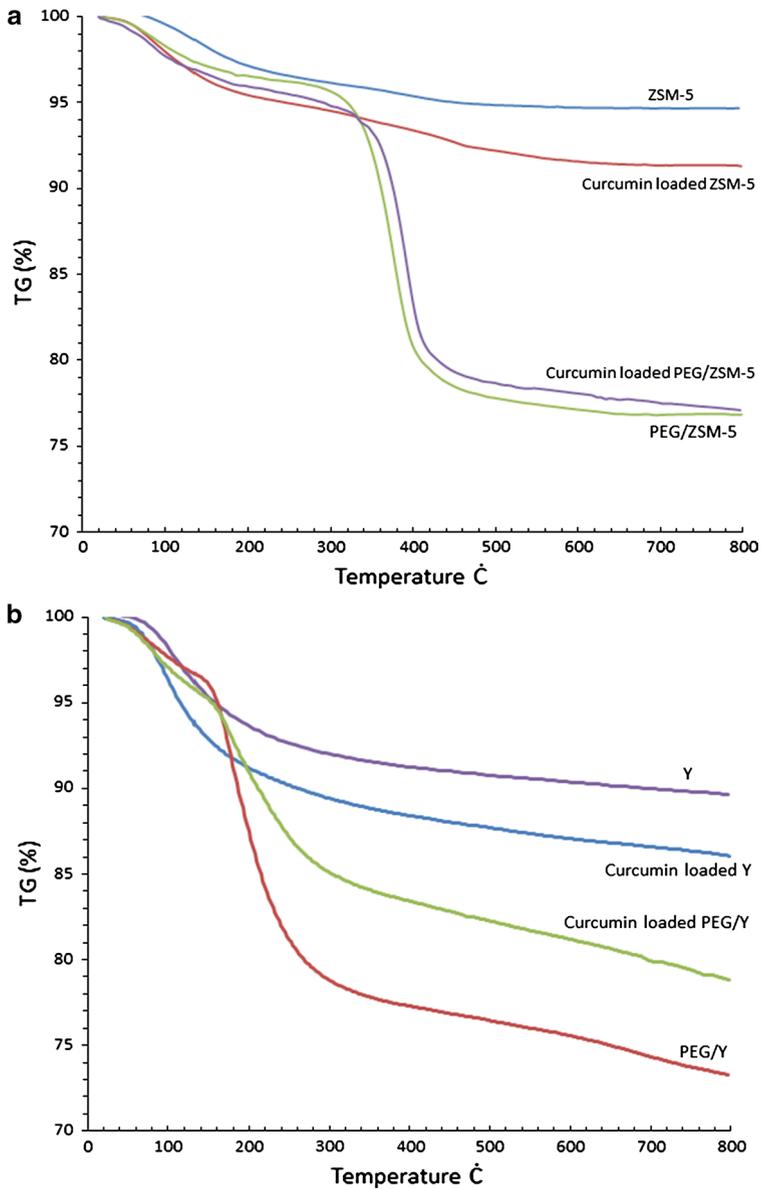
Fig. 3 TGA for: **a** zeolite ZSM-5, curcumin-loaded ZSM-5, PEG/ZSM-5, curcumin-loaded PEG/ZSM-5; **b** zeolite Y, curcumin-loaded Y, PEG/Y, curcumin-loaded PEG/Y

TG analysis

Thermogravimetric analysis (TGA) enables investigation of the properties of a sample as a function of temperature. TGA is a commonly used technique in the polymer science

to monitor polymer thermal behavior. In this study, thermal gravimetry was used in an attempt to understand the extent of surface modification of zeolites with PEG. Besides, thermal analysis of drug-loaded zeolite samples could also provide valuable information about the extent of payload drug into carriers. Figure 3a shows the TGA curves of the ZSM-5, curcumin-loaded ZSM-5, PEG/ZSM-5 and curcumin-loaded PEG/ZSM-5. It is believed that the decomposition of PEG takes place in the range of 140–450 °C; consequently, the mass loss of 18.17% wt at the same range for PEG/ZSM-5 nanocomposite can confirm the successful synthesis of ZSM-5/PEG nanocomposite. Considering the decomposition temperature of curcumin reported to be around 200 °C [32] and the corresponding observed mass loss in the curcumin-loaded ZSM-5, the results show that the drug content in the ZSM-5 zeolite was about 3.37% wt. In case of TGA curve of curcumin-loaded PEG/ZSM-5, due to overlapping of curcumin and PEG degradation temperature range, it is not possible to determine exact curcumin and PEG amounts solely. The results revealed that the amount of weight loss in the temperature range of 140–480 °C was about 17.33% wt which relates to the both curcumin and PEG decomposition. The reason behind the decrease in the polymer content for curcumin-loaded PEG/ZSM-5 compared to the PEG/ZSM-5 nanocomposite can be explained by losing some part of PEG by dissolving in ethanol during the drug loading process.

Figure 3b shows the TGA analyze of the zeolite Y, curcumin-loaded zeolite Y, PEG/Y nanocomposite and curcumin-loaded PEG/Y. As it can be seen, the weight loss of 3.62% in the temperature around 200 °C is related to the amount of curcumin loaded into Y zeolite. For PEG/Y nanocomposite, PEG content was about 18.73% wt. TGA curve of the curcumin-loaded PEG/Y demonstrates the sample weight in the temperature range of 140–480 °C corresponding to the curcumin, and PEG was decreased by 12.68%. The same explanation of curcumin-loaded PEG/ZSM-5 is applicable for the decrease in PEG amount in curcumin-loaded PEG/Y compared to the PEG/Y nanocomposite.

Zeta potential

Zeta potential can provide some information about the chemical nature and the surface characteristic of particles. Originally, both zeolites possessed relatively high negative charge of about -16 ± 0.9 and -14.3 ± 1.6 mV for zeolite Y and ZSM-5, respectively, which arises from their aluminosilicate framework. Clearly, high negative charge is an important parameter in formation of stable dispersion which is critical for being used in biomedical applications. As expected, decoration of the surface of zeolites with PEG caused a little decrease in the corresponding surface charge, providing a supportive evidence for nanocomposite formation. The zeta potential of zeolite Y/PEG

Table 1 Zeta potential of Y, ZSM-5, PEG/Y and PEG/ZSM-5

Zeolite/nanocomposite	Y zeolite	ZSM-5 zeolite	PEG/Y	PEG/ZSM-5
Zeta potential (mV)	-16 ± 0.9	-14.3 ± 1.6	-13.8 ± 0.6	-12.1 ± 1.1

changed from -16 ± 0.9 to -13.8 ± 0.6, and for ZSM-5 it changed from -14.3 ± 1.6 to -12.1 ± 1.1 mV. The data are reported in Table 1.

BET analysis

The BET analysis is widely considered as a powerful technique to determine surface areas of different metal–organic frameworks like zeolites. The surface area and pore volume data of the ZSM-5 samples (ZSM-5 zeolite, curcumin-loaded ZSM-5, PEG/ZSM-5 and curcumin-loaded PEG/ZSM-5) and Y zeolite samples (Y zeolite, curcumin-loaded Y, PEG/Y and curcumin-loaded PEG/Y) are given in Table 2. Generally, all zeolites before drug loading exhibited a large specific surface area, typically more than 486 and 66 m^2 g^{-1} for zeolite Y and ZSM-5, respectively, with most of this area being internal (void volume above 0.50 and 0.1 cm^3 g^{-1}, respectively). As it can be seen, drug loading decreased the surface areas and the pore volumes, confirming curcumin inclusion in the pores of the samples. Besides, a high decrease in the surface area and pore volume occurred after both nanocomposite synthesis can be presumably explained by closing the pores of zeolites by PEG and subsequently preventing N_2 gas to go inside which is similar to the results of previous reports [11, 33]. The surface area and pore volume in drug-loaded PEG/ZSM-5 were higher than in PEG/ZSM-5 which could further support the explanation for TGA that some extent of PEG is removed during drug loading process.

SEM

Figure 4a shows SEM images of the ZSM-5 samples (ZSM-5, curcumin-loaded ZSM-5 and PEG/ZSM-5). As shown, the SEM results reveal that curcumin in the all zeolite samples is located in the empty space within the structure of ZSM-5 zeolite which is consistent with the BET results. SEM image of PEG/ZSM-5 shows that the surface of the ZSM-5 zeolite is covered by PEG, and these images correspond well with the results of BET analysis. Figure 4b shows SEM images of the Y samples

Table 2 BET data for different samples

Zeolite	Samples	Surface area (m^2/g)	Total pore volume (cm^3/g)
ZSM-5	ZSM-5	66.045	0.194
	Curcumin-loaded ZSM-5	19.73	0.191
	PEG/ZSM-5	8.091	0.0671
	Curcumin-loaded PEG/ZSM-5	9.076	0.0806
Y	Y	489.57	0.538
	Curcumin-loaded Y	327.97	0.4928
	PEG/Y	43.05	0.2103
	Curcumin-loaded PEG/Y	83.356	0.3203
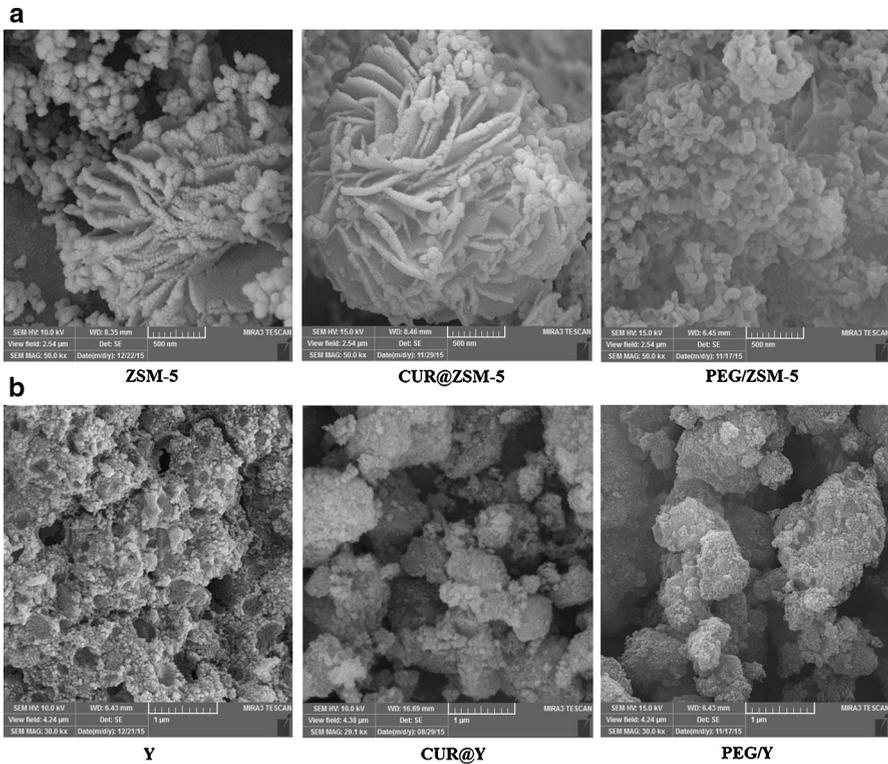
Fig. 4 SEM images for: **a** ZSM-5, curcumin-loaded ZSM-5, PEG/ZSM-5; **b** Y, curcumin-loaded Y, PEG/Y

(zeolite Y, curcumin-loaded Y and PEG/Y). The explanation for these images is similar to that of ZSM-5 zeolite samples. Also, in these images, empty spaces of Y zeolite are filled with PEG and curcumin [9, 34].

Characterization of host–guest system

Curcumin, considering its molecular size and structure, is expected to be an adequate candidate as a guest for being loaded into the zeolite pores as host. Zeolites owing to the pore size less than 20 Å which is close to the size of many bioactive molecules are good candidate as drug delivery systems. In this study, curcumin was loaded into two different types of zeolites (Y and ZSM-5) with diverse frameworks and pore sizes in order to investigate the impact of zeolite framework on the characteristics of these materials as carrier for controlled drug delivery system.

The extent of curcumin encapsulation in the different zeolite samples including zeolite Y, ZSM-5, PEG/Y and PEG/ZSM-5 was determined to be 60.06%, 40.45%, 45.59% and 37.46%, respectively. Clearly, zeolite Y possesses the highest capability to load drug with drug encapsulation efficiency of about 60.06% followed by PEG/Y

(45.59%), ZSM-5 (40.45%) and PEG/ZSM-5 (37.46%). It is not surprising that considering the results of BET analysis, zeolite Y revealed the highest total pore volume than the ZSM-5 zeolite and consequently the highest capacity for guest inclusion; the results are consistent with the previous studies [10, 12]. Besides, the amount of encapsulated curcumin in the nanocomposite hosts was less than in the zeolite hosts because of the coverage of zeolites surface by PEG. These results are consistent with the results of TGA and BET analysis. It is worth saying that although the presence of PEG decreases the pore volume and subsequently decreases the drug encapsulation, it plays a determinant role in the application of zeolites as a drug carrier considering its influence in controlled drug release, dispersibility of zeolite, decrease in reticuloendothelial system (RES) uptake, immunogenicity, and enhanced biocompatibility of zeolite.

Drug release study

Considering the impact of the host–guest chemical interaction and pore size on the drug release profile, the type of zeolite framework and the surface modification is expected to show a crucial impact on controlling the delivery rate of the guest drug. The release profiles of curcumin from ZSM-5 zeolite and PEG/ZSM-5 nanocomposite at different pH values of 7.4, and 5.4 are shown in Fig. 5. As shown, maximum attainable amount of drug release for ZSM-5 and PEG/ZSM-5 at pH of 7.4 was only 3 and 6% up to 100 h, respectively. Figure 6 shows curcumin release from Y zeolite and PEG/Y nanocomposite at different pH values of 7.4 and 5.4. The maximum extent of drug release for Y zeolite and PEG/Y at pH of 7.4 was about 5 and 16%, which was achieved in 96 and 120 h, respectively. As it can be seen, it is obvious that both zeolites show low extent of initial burst rates of drug release
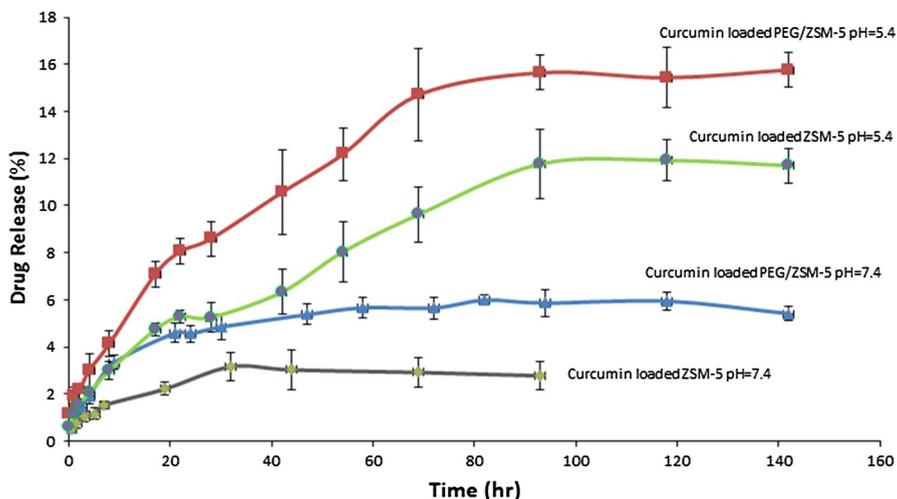
Fig. 5 Curcumin release from curcumin-loaded ZSM-5 and curcumin-loaded PEG/ZSM-5 at different pH values. PEG/ZSM-5 pH = 5.4, ZSM-5 pH = 5.4, PEG/ZSM-5 pH = 7.4, ZSM-5 pH = 7.4
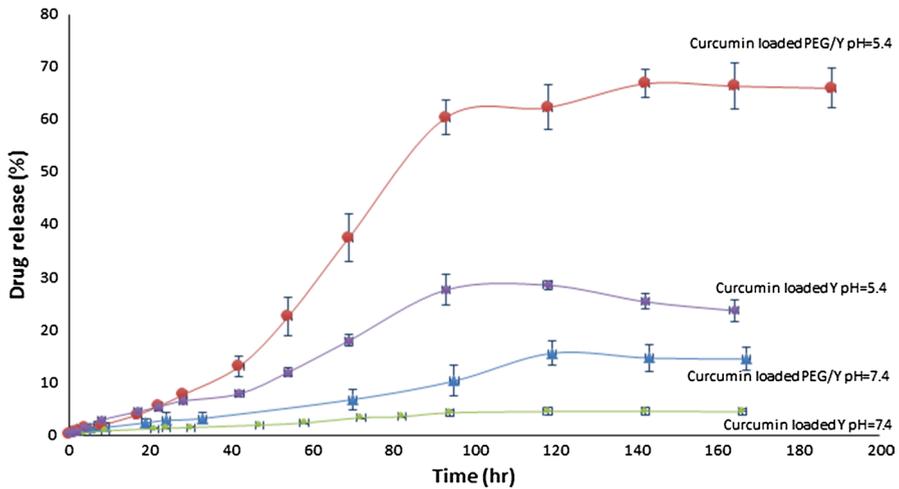
Fig. 6 Curcumin release from curcumin-loaded Y and curcumin-loaded PEG/Y at different pH values. PEG/Y pH=5.4, Y zeolite pH=5.4, PEG/Y pH=7.4, Y zeolite pH=7.4

with an exponential-type behavior. But the amount of drug release for Y zeolite was higher than for corresponding ZSM-5, maybe due to its higher pore volume and its interactions with the drug. Curcumin is a small molecule with molecular dimensions 5.2×5.9 A°, which can easily diffuse out of the micropores of faujasite and results in the enhanced release of the drug. On the other hand, ZSM-5 zeolite has smaller pore diameter than Y zeolite which is very close to curcumin size so it makes it difficult for curcumin to be diffused out and released. Consequently, the diffusion from the zeolite pores and channels appears to influence drug release pattern. Besides, there is a slight increase in drug release for nanocomposites compared to the zeolites which can be related to the increased solubility of curcumin in the presence of PEG.

The profile of curcumin release from different carriers in acidic environment is of great importance because of lower physiological pH environment (pH 5–5.5) present in the endosomes of the cancer cells compared to the normal cells and is widely used as a promising passive approach to developing different targeted delivery systems. To examine the validity of this approach, the release behavior of the drug from various zeolites of interest was examined in buffer solutions with the pH value of 5.4. Figure 5 illustrates the release profile of curcumin from ZSM-5 zeolite and PEG/ZSM-5 nanocomposite at the pH value of 5.4. In fact, the amount of curcumin released at pH=5.4 is higher than at pH=7.4, especially in the case of PEG/ZSM-5. In acidic medium, the extent of drug release for PEG/Y (67%) was dramatically higher than for zeolite Y (29%) which can be attributed to the curcumin interaction with zeolite in the acidic media probably due to enhanced solubility of curcumin in acidic environment and weakened the physical interaction particularly hydrogen bonding between curcumin and zeolite hosts. It can be expected that this sustained release of curcumin will maintain a constant exposure of drug to the cancer cell, resulting in enhanced anticancer effect and benefits for drug delivery applications [35].

Drug release kinetic

The various kinetic equations including zero-order model, first-order model, second-order model, Higuchi model, Hixson–Crowell model, Korsmeyer–Peppas model and Kopcha model are used to fit the release data of zeolites [36]. The corresponding kinetic data for curcumin release from ZSM-5, PEG/ZSM-5, Y and PEG/Y for both pH values 7.4 and 5.4 are summarized in Table 3. The model with the highest correlation coefficients (R^2) was chosen as the best fit. Data analysis was performed using the Excel add-in DDSolver program. As reported in Table 3, Korsmeyer–Peppas model showed the best fit model for most systems, indicating that diffusion is the most dominant mechanism for both types of zeolites and PEG-modified zeolites.

DPPH radical scavenging activity

The antioxidant activity of various carriers was determined by DPPH free radical scavenging assay which was based on the reduction of radical DPPH in alcoholic solution [37]. The results of the DPPH scavenging ability of the curcumin, curcumin-loaded ZSM-5, curcumin-loaded Y, curcumin-loaded PEG/ZSM-5 and curcumin-loaded PEG/Y are shown in Fig. 7. Curcumin has the most antioxidant activity, and the curcumin-loaded PEG/ZSM-5 showed more potential of antioxidant activity than the curcumin-loaded ZSM-5. Curcumin-loaded PEG/Y has also higher antioxidant activities than curcumin-loaded Y. These results can be explained according to the findings in the release study where the presence of PEG in the carrier structure increased the extent of drug released which in turn could simply increase the antioxidant properties of carrier.

Conclusion

Different types of zeolites, i.e., Y and ZSM-5 as well as their corresponding nanocomposite of PEG (PEG/Y and PEG/ZSM-5), were used as carrier for loading and release of curcumin. Zeolites and PEG/zeolite nanocomposites were characterized by XRD, SEM and FT-IR techniques. Curcumin encapsulation efficiency of Y, ZSM-5, PEG/Y and PEG/ZSM-5 was determined to be 61.06, 40.45, 45.59 and 37.76%, respectively. Nitrogen adsorption–desorption results indicating a decrease in the surface areas and pore volumes of host after drug loading confirmed the inclusion of curcumin in the zeolites pores. In vitro drug release of curcumin was studied in buffer solution (pH = 5.4 and 7.4) at 37 °C. The results showed higher levels of curcumin release from zeolite Y compared to ZSM-5. The zeolite nanocomposites also revealed the higher level of released curcumin in comparison with the corresponding zeolites. The amount of curcumin released at pH = 5.4 was higher than at pH = 7.4, which can be used as evidence to demonstrate the pH sensitivity of the zeolite as drug carrier. From the results, it can be concluded that zeolite-based drug

Table 3 Parameters set of mathematical models and correlation coefficient

Host	pH	Zero-order $Qt=Q_0+K_0t$	First-order $LnQt=LnQ_0+K_1t$	Second-order $Qt/Q\infty(Q\infty-Qt)=K_2t$	Higuchi $Qt=KH\sqrt{t}$	Kopcha $Mt=A\sqrt{t}+Bt$	Hixson–Crowell $W_t(1/3)=-Kst+W_0(1/3)$	Korsmeyer–Peppas $Log\,Mt/M\infty=Log\,a+nLog\,t$
ZSM-5	5.4	R2: 0.90 K0: 0.0003	R2: 0.67 K1: 0.017	R2: 0.01 K2: −4.24	R2: 0.98 KH: 0.0039	R2: 0.90 A: 0.0039 B: $7.67\times10-6$	R2: 0.91 KS: −0.0002	R2: 0.98 n: 0.54 a: 0.0784
	7.3	R2: 0.53 K0: 0.0001	R2: 0.56 K1: 0.015	R2: 0.21 K2: 35,078	R2: 0.81 KH: 0.0011	R2: 0.62 A: 0.001,223 B: $1.74\times10-5$	R2: 0.62 KS: $-6\times10-5$	R2: 0.95 n: 0.37 a: 0.24
PEG/ZSM-5	5.4	R2: 0.84 K0: 0.0004	R2: 0.84 K1: 0.0004	R2: 0.85 K2: 0.0015	R2: 0.97 KH: 0.0047	R2: 0.84 A: 0.004649 B: $3.74\times10-5$	R2: 0.85 KS: 0.0003	R2: 0.98 n: 0.51 a: 0.096
	7.3	R2: 0.60 K0: 0.0001	R2: 0.47 K1: 0.011	R2: 0.04 K2: −2368	R2: 0.81 KH: 0.0016	R2: 0.60 A: 0.001883 B: $1.61\times10-5$	R2: 0.60 KS: $-8\times10-5$	R2: 0.93 n: 0.41 a: 0.17
Zeolite Y	5.4	R2: 0.87 K0: 0.001	R2: 0.70 K1: 0.022	R2: 0.11 K2: 7827	R2: 0.89 KH: 0.013	R2: 0.87 A: 0.005996 B: $5.40\times10-4$	R2: 0.87 KS: −0.0006	R2: 0.99 n: 0.81 a: 0.0175
	7.3	R2: 0.92 K0: 0.0002	R2: 0.79 K1: 0.015	R2: 0.19 K2: 11,134	R2: 0.96 KH: 0.0022	R2: 0.92 A: 0.000763 B: $1.08\times10-4$	R2: 0.92 KS: $-8\times10-5$	R2: 0.95 n: 0.48 a: 0.083
PEG/Y	5.4	R2: 0.92 K0: 0.0018	R2: 0.76 K1: 0.026	R2: 0.49 K2: −4.074	R2: 0.90 KH: 0.025	R2: 0.92 A: 0.00324 B: $1.50\times10-3$	R2: 0.93 KS: −0.0015	R2: 0.96 n: 1.02 a: 0.0055
	7.3	R2: 0.96 K0: 0.0004	R2: 0.91 K1: 0.017	R2: 0.02 K2: −1.29	R2: 0.92 KH: 0.0052	R2: 0.96 A: 0.000235 B: $3.92\times10-4$	R2: 0.95 KS: −0.0002	R2: 0.89 n: 0.51 a: 0.054
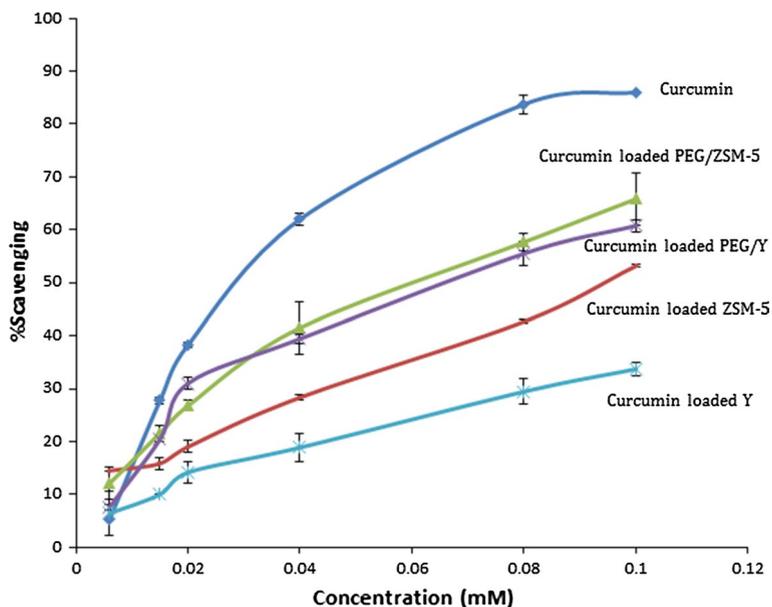
Fig. 7 DPPH radical scavenging activity for: **a** curcumin, curcumin-loaded PEG/ZSM-5, curcumin-loaded PEG/Y, curcumin-loaded ZSM-5 and curcumin-loaded Y

delivery systems can be considered as promising candidate for delivery of hydrophobic drugs such as curcumin.

References

1. Ji SH, Cho JH, Jeong YH, Do Yun J, Yun JS (2017) The synthesis of flexible zeolite nanofibers by a polymer surface thermal etching process. Appl Surf Sci 416:178–182
2. Wang L, Yang H, Pan G, Miao L, Chen S, Song Y (2017) Polyaniline–carbon nanotubes@ zeolite imidazolate framework67-carbon cloth hierarchical nanostructures for supercapacitor electrode. Electrochim Acta 240:16–23
3. Benyakhou S, Belmokhtar A, Zehhaf A, Benyoucef A (2017) Development of novel hybrid materials based on poly (2-aminophenyl disulfide)/silica gel: preparation, characterization and electrochemical studies. J Mol Struct 1150:580–585
4. Benykhlef S, Bekhoukh A, Berenguer R, Benyoucef A, Morallon E (2016) PANI-derived polymer/Al2O3 nanocomposites: synthesis, characterization, and electrochemical studies. Colloid Polym Sci 294(12):1877–1885
5. Chouli F, Radja I, Morallon E, Benyoucef A (2017) A novel conducting nanocomposite obtained by p-anisidine and aniline with titanium (IV) oxide nanoparticles: synthesis, characterization, and electrochemical properties. Polym Compos 38:E254–E260
6. Barbe C, Bartlett J, Kong L, Finnie K, Lin HQ, Larkin M et al (2004) Silica particles: a novel drug-delivery system. Adv Mater 16(21):1959–1966

7. Costa R, Ribeiro C, Lopes A, Martins P, Sencadas V, Soares R et al (2013) Osteoblast, fibroblast and in vivo biological response to poly (vinylidene fluoride) based composite materials. J Mater Sci Mater Med 24(2):395–403

8. Petushkov A, Ndiege N, Salem AK, Larsen SC (2010) Toxicity of silica nanomaterials: zeolites, mesoporous silica, and amorphous silica nanoparticles. Adv Mol Toxicol 4:223–266

9. Khodaverdi E, Honarmandi R, Alibolandi M, Baygi RR, Hadizadeh F, Zohuri G (2014) Evaluation of synthetic zeolites as oral delivery vehicle for anti-inflammatory drugs. Iran J Basic Med Sci 17(5):337–343

10. Dyer A, Morgan S, Wells P, Williams C (2000) The use of zeolites as slow release anthelmintic carriers. J Helminthol 74(2):137–141 **PubMed PMID: 10881284**

11. Khodaverdi E, Soleimani HA, Mohammadpour F, Hadizadeh F (2016) Synthetic zeolites as controlled-release delivery systems for anti-inflammatory drugs. Chem Biol Drug Des 87(6):849–857 **PubMed PMID: 26705687**

12. Amorim R, Vilaça N, Martinho O, Reis RM, Sardo M, Rocha J et al (2012) Zeolite structures loading with an anticancer compound as drug delivery systems. J Phys Chem C 116(48):25642–25650

13. Horcajada P, Rámila A, Pérez-Pariente J, Vallet Regi M (2004) Influence of pore size of MCM-41 matrices on drug delivery rate. Microporous Mesoporous Mater 68(1):105–109

14. Serri C, de Gennaro B, Quagliariello V, Iaffaioli RV, De Rosa G, Catalanotti L et al (2017) Surface modified zeolite-based granulates for the sustained release of diclofenac sodium. Eur J Pharm Sci 99:202–208

15. Salim MM, Malek NANN (2016) Characterization and antibacterial activity of silver exchanged regenerated NaY zeolite from surfactant-modified NaY zeolite. Mater Sci Eng C 59:70–77

16. Serri C, de Gennaro B, Quagliariello V, Iaffaioli RV, De Rosa G, Catalanotti L et al (2017) Surface modified zeolite-based granulates for the sustained release of diclofenac sodium. Eur J Pharm Sci 01(99):202–208 **PubMed PMID: 28012939**

17. Zhang H, Kim Y, Dutta PK (2006) Controlled release of paraquat from surface-modified zeolite Y. Microporous Mesoporous Mater 88(1):312–318

18. Hussein MA, Abu-Zied BM, Asiri AM (2014) Preparation, characterization, and electrical properties of ZSM-5/PEG composite particles. Polym Compos 35(6):1160–1168

19. Zou Y, Lu Y, Wei D (2004) Antioxidant activity of a flavonoid-rich extract of Hypericum perforatum L. in vitro. J Agric Food Chem 52(16):5032–5039

20. Abu-Zied BM, Schwieger W, Unger A (2008) Nitrous oxide decomposition over transition metal exchanged ZSM-5 zeolites prepared by the solid-state ion-exchange method. Appl Catal B 84(1):277–288

21. Feng L, Zhao W, Zheng J, Frisco S, Song P, Li X (2011) The shape-stabilized phase change materials composed of polyethylene glycol and various mesoporous matrices (AC, SBA-15 and MCM-41). Sol Energy Mater Sol Cells 95(12):3550–3556

22. Feng L, Zheng J, Yang H, Guo Y, Li W, Li X (2011) Preparation and characterization of polyethylene glycol/active carbon composites as shape-stabilized phase change materials. Sol Energy Mater Sol Cells 95(2):644–650

23. Li H, Fang GY (2010) Experimental investigation on the characteristics of polyethylene glycol/cement composites as thermal energy storage materials. Chem Eng Technol 33(10):1650–1654

24. Zhang L, Zhu J, Zhou W, Wang J, Wang Y (2011) Characterization of polymethyl methacrylate/polyethylene glycol/aluminum nitride composite as form-stable phase change material prepared by in situ polymerization method. Thermochim Acta 524(1):128–134

25. Zhang L, Zhu J, Zhou W, Wang J, Wang Y (2012) Thermal and electrical conductivity enhancement of graphite nanoplatelets on form-stable polyethylene glycol/polymethyl methacrylate composite phase change materials. Energy 39(1):294–302

26. Salman N, Rüscher C, Buhl J-C, Lutz W, Toufar H, Stöcker M (2006) Effect of temperature and time in the hydrothermal treatment of HY zeolite. Microporous Mesoporous Mater 90(1):339–346

27. Anitha A, Deepagan V, Rani VD, Menon D, Nair S, Jayakumar R (2011) Preparation, characterization, in vitro drug release and biological studies of curcumin loaded dextran sulphate–chitosan nanoparticles. Carbohydr Polym 84(3):1158–1164

28. Morales-Pacheco P, Domínguez J, Bucio L, Alvarez F, Sedran U, Falco M (2011) Synthesis of FAU (Y)-and MFI (ZSM5)-nanosized crystallites for catalytic cracking of 1, 3, 5-triisopropylbenzene. Catal Today 166(1):25–38

29. Cejka J, Van Bekkum H, Corma A, Schueth F (2007) Introduction to zeolite molecular sieves. Elsevier, Amsterdam

30. Cheng Y, Wang L-J, Li J-S, Yang Y-C, Sun X-Y (2005) Preparation and characterization of nano-sized ZSM-5 zeolites in the absence of organic template. Mater Lett 59(27):3427–3430

31. Wang W, Yang X, Fang Y, Ding J (2009) Preparation and performance of form-stable polyethylene glycol/silicon dioxide composites as solid–liquid phase change materials. Appl Energy 86(2):170–174

32. Mathew A, Fukuda T, Nagaoka Y, Hasumura T, Morimoto H, Yoshida Y et al (2012) Curcumin loaded-PLGA nanoparticles conjugated with Tet-1 peptide for potential use in Alzheimer's disease. PLoS ONE 7(3):e32616

33. Rimoli MG, Rabaioli MR, Melisi D, Curcio A, Mondello S, Mirabelli R et al (2008) Synthetic zeolites as a new tool for drug delivery. J Biomed Mater Res Part A 87(1):156–164

34. Fatouros DG, Douroumis D, Nikolakis V, Ntais S, Moschovi AM, Trivedi V et al (2011) In vitro and in silico investigations of drug delivery via zeolite BEA. J Mater Chem 21(21):7789–7794

35. Ren H, Zhang L, An J, Wang T, Li L, Si X et al (2014) Polyacrylic acid@ zeolitic imidazolate framework-8 nanoparticles with ultrahigh drug loading capability for pH-sensitive drug release. Chem Commun 50(8):1000–1002

36. Ainurofiq A, Choiri S (2015) Drug release mechanism of slightly soluble drug from nanocomposite matrix formulated with zeolite/hydrotalcite as drug carrier. Trop J Pharm Res 14(7):1129–1135

37. Khalkhali M, Sadighian S, Rostamizadeh K, Khoeini F, Naghibi M, Bayat N et al (2015) Synthesis and characterization of dextran coated magnetite nanoparticles for diagnostics and therapy. BioImpacts BI 5(3):141